Anal. Calcd for $C_6H_{12}F_6Ge_2$: C, 26.2; H, 3.2. Found: C, 26.6; H, 2.9.

Preparation of 1,1,4,4-Tetramethyl-2,5-di-*tert*-butyl-1,4-digermacyclohexa-2,5-diene (4g) and 1,1-Dimethyl-2,4-di-*tert*-butyl-1-germacyclopenta-2,4-diene (6c): 1.0 g (1.9 mmol) of **2**, 0.47 g (5.7 mmol) of **3e**, 0.3 g (0.26 mmol) of $Pd(PPh_3)_4$, 10 mL of benzene, T = 72 °C, t = 4 h, bp 140 °C/0.01 Torr, ratio 8:2 **4g:6c**; **6c** ^{1}H NMR ($CDCl_3$) δ 0.40 (s, $GeCH_3$, 6 H), 1.08, 1.10 (each s, tBu, each 9 H), 5.48 (s, HC=, 1 H), 5.73 (s, HC=, 1 H), GC-MS (relative intensity) m/e 268 (21, M^+), 149 (100, M^+ - $GeMe_3$). **4g** ^{1}H NMR ($CDCl_3$) δ 0.33 (s, 12 H, $GeCH_3$), 1.07 (s, tBu, 18 H), 6.37 (s, HC=, 2 H), ^{13}C NMR ($CDCl_3$) δ 2.61 ($GeCH_3$), 30.28 (CH_3, tBu), 39.76 (Cq, tBu), 137.26 (HC=), 168.82 (C=, Cq), GC-MS (relative intensity) m/e 370 (20, M^+), 355 (100, M^+ - Me).

Preparation of the Germoles 6d-j: 1.0 g (1.9 mmol) of **2**, 5.7 mmol of **3a,m,n**; 4.0 mmol of **3l**, 6.0 mmol of **3j**, 0.3 g (0.26 mmol) of $Pd(PPh_3)_4$, 10 mL of benzene, ratio **6d:6e,f** (>90% **6d**); **6d** bp 100 °C/0.02 Torr, ^{1}H NMR ($CDCl_3$) δ 0.43 (s, $GeCH_3$, 6 H), 1.02 (m, CH_3, 6 H), 1.50 (m, CH_2, 8 H), 2.35 (m, CH_2, 4 H), 5.67 (m, HC=, 1 H, ^4J(H-H) = 1.2 Hz), 6.33 (m, HC=, 1 H, ^4J(H-H) = 1.2 Hz), GC-MS (relative intensity) m/e 268 (43, M^+), 121 (100, C_9H_{13}); **6e,f** GC-MS m/e 268 (69, M^+), 105 (100, $GeMe_2H$), 269 (100, M^+); **6g** bp 130 °C/0.01 Torr, ^{1}H NMR ($CDCL_3$) δ 0.55 (s, 6 H, $GeCH_3$), 2.35 (s, 6 H, CH_3), 6.23 (d, 1 H, HC:, ^4J(H-H) = 1.2 Hz), 6.83 (d, 1 H, HC=), 7.17 (m, 8 H, Ph), ^{13}C NMR ($CDCl_3$) -2.83 ($GeCH_3$), 20.49, 21.43 (CH_3), 125.59, 125.65, 126.04, 127.16, 128.32, 129.50, 129.73, 130.19, 130.36, 132.01 (CH, Ph), 135.00, 140.01, 140.91, 141.59, 141.68, 155.90 (Cq), GC-MS m/e (relative intensity) 336 (83, M^+), 89 (100, GeMe); **6h** bp 130 °C/0.02 Torr, ^{1}H NMR ($CDCl_3$) 0.56 (s, 6 H, $GeCH_3$), 2.13, 2.40 (each s, each 3 H, CH_3), 3.78, 3.93 (each s, CH_3, each 3 H), ^{13}C NMR ($CDCl_3$) δ -4.38 ($GeCH_3$), 16.86, 17.53 (CH_3), 51.15, 51.52 ($COCH_3$), 128.24, 144.21, 154.57, 160.17 (Cq), 167.77, 167.97 (CO, Cq), GC-MS (relative intensity) m/e 300 (63, M^+), 105 (100, GeMeO); **6i** bp 200 °C/0.01 Torr, ^{1}H NMR ($CDCl_3$) δ 0.73 (s, 6 H, $GeCH_3$), 0.82, 1.09 (each t, each 3 H, CH_3, ^3J(H-H) = 7.2 Hz), 3.82, 4.03 (each q, each 2 H, CH_2), 7.30 (m, Ph, 10 H), ^{13}C NMR ($CDCl_3$) δ -3.12 ($GeCH_3$), 13.28, 13.80 (CH_3), 59.68, 60.42 (CH_2), 126.87, 127.04, 127.28, 127.50, 128.19, 128.32 (CH, Ph), 137.42, 137.57, 137.82, 143.28, 151.94, 159.78 (Cq), 166.33, 167.29 (CO, Cq), GC-MS (relative intensity) m/e 407 (29, M^+ - OEt), 105 (100, GeMeO); **6j** ^{1}H NMR ($CDCl_3$) δ 0.60 (s, 6 H, $GeCH_3$), 6.78 (m, 10 H, Ph), HRMS (EI) m/e calcd for M^+ ($C_{30}H_{26}Ge$) 460.1279, found 460.1260, mp 178 °C (179-180 °C).[21] Anal. Calcd for $C_{30}H_{26}Ge$: C, 78.4; H, 5.7. Found: C, 78.5; H, 5.7.

Acknowledgment. This research has been supported by the Fonds der Chemischen Industrie. We thank Dr. H. Hillgärtner and Mr. P. Urschel for skillful help in complicated MS and HRMS measurements and Professor Dr. J. Broekaert and Mr. M. Hüffner for special attention to and patience with elemental analyses.

Supplementary Material Available: ^{1}H and ^{13}C NMR spectra for **5a,c,f** and **7** and ^{13}C NMR spectra for **4a,b** (9 pages). Ordering information is given on any current masthead page.

OM910324J

(21) Hota, N. K.; Willis, C. J. *J. Organomet. Chem.* **1968**, *15*, 89.

Chelate Control of Diphosphines around Platinum(II): η^2-Cyclenphosphoranide-Promoted Formation of Heterobimetallics

Dilip V. Khasnis, Michael Lattman,* Upali Siriwardane,[1] and Hongming Zhang

Department of Chemistry, Southern Methodist University, Dallas, Texas 75275

Received December 5, 1991

The presence of the three-membered ring (containing nitrogen, phosphorus, and platinum) in (η^2-cyclenP)Pt square-planar complexes inhibits chelation of another small-bite bidentate ligand. Thus, (η^2-cyclenP)Pt(Cl)PPh_3 (**1**) reacts with dppe to form the bisbidentate derivative [(η^2-cyclenP)Pt(η^2-$Ph_2P(CH_2)_2PPh_2$)]Cl (**2a**), while previous work showed that reaction with dppm yielded (η^2-cyclenP)Pt(Cl)$Ph_2PCH_2PPh_2$ (**3**), where only one end of dppm is coordinated. Displacement of chloride from **3** by addition of $NaBPh_4$ leads to a mixture of compounds, one of which does appear to be the bischelate species [(η^2-cyclenP)Pt(η^2-$Ph_2PCH_2PPh_2$)]BPh_4 (**4**). Treatment of **3** with HBF_4 results in cleavage of the three-membered ring to give pure [(H_2cyclenP)Pt(Cl)(η^2-$Ph_2PCH_2PPh_2$)]$(BF_4)_2$ (**5**) in which dppm is bidentate. Restricting dppm to monodentate is useful in the formation of bridged heterobimetallic complexes with direct metal-metal bonds as shown by the reaction of **3** with Na[$Co(CO)_4$], which leads to (η^2-cyclenP)Pt[$Co(CO)_3$](μ-$Ph_2PCH_2PPh_2$) (**6**). X-ray data for **5**: $C_{33}H_{40}N_4P_3ClPt\cdot 2BF_4\cdot CH_3CN$, a = 16.113 (4) Å, b = 13.194 (5) Å, c = 20.500 (8) Å, β = 109.82 (3)°, monoclinic $P2_1/n$, Z = 4. X-ray data for **6**: $C_{36}H_{38}N_4O_3P_3CoPt\cdot C_6H_6$, a = 12.119 (4) Å, b = 24.840 (8) Å, c = 13.919 (4) Å, β = 103.20 (2)°, monoclinic $P2_1/n$, Z = 4.

Diphosphines, $R_2P(CH_2)_nPR_2$, are very common and important chelating and bridging ligands in transition-metal chemistry. The ability to initially restrict binding of these ligands to only one donor atom is potentially useful in the design of heterobimetallics. Thus far, coordination of only one end of a diphosphine has been accomplished by (1) using excess ligand to displace one end of the chelating diphosphine, (2) incorporating nonlabile ligands onto the metal, and (3) constraining the metal to undergo trans substitution only.[2] Our investigations into the chemistry of η^2-cyclenP square-planar complexes[3] suggest that an-

(1) Present address: Louisiana Tech University.

(2) See, for example: (a) Puddephatt, R. J. *Chem. Soc. Rev.* **1983**, *99*. (b) Chaudret, B.; Delavaux, B.; Poilblanc, R. *Coord. Chem. Rev.* **1988**, *86*, 191.

0276-7333/92/2311-2074$03.00/0

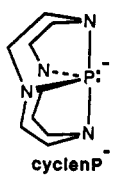

cyclenP⁻

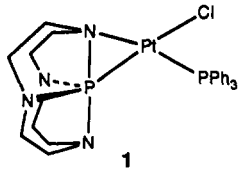

1

other way exists: one small-bite ligand may inhibit chelation of a second small-bite ligand. We herein report that the reactions of the phosphoranide (R_4P^-) complex (η^2-cyclenP)Pt(Cl)PPh_3 (1) with $Ph_2P(CH_2)_nPPh_2$ [dppe (n = 2) and dppm (n = 1)] yield different products, apparently due to the combination of the constraint of the three-membered ring of the cyclenP ligand and the smaller bite angle of chelated dppm compared with dppe. In addition, we demonstrate the utility of this ring constraint in the synthesis of a species with a dppm-bridged platinum–cobalt bond.

Experimental Section

All reactions and manipulations were carried out under an atmosphere of nitrogen in a Vacuum Atmospheres Model DL-001-S-P drybox or using standard Schlenk techniques, unless otherwise indicated. Solvents were dried and distilled under a nitrogen atmosphere and either used immediately or stored in the drybox prior to use. Glassware was oven-dried at 140 °C overnight prior to use. The reagents dppe, dppm, $NaPF_6$, $NaBPh_4$, 85% $HBF_4{\cdot}O(C_2H_5)_2$, and $Co_2(CO)_8$ were obtained commercially and used without further purification except for $Co_2(CO)_8$, which was sublimed prior to use; compounds 1[3b] and 3[3d] were prepared by literature methods. All NMR spectra were recorded on an IBM/Bruker WP200SY multinuclear NMR spectrometer resonating at 200.132 (^{1}H) and 81.026 (^{31}P)MHz. ^{31}P spectra are proton-decoupled unless otherwise indicated. ^{1}H resonances were measured relative to residual proton solvent peaks and referenced to Me_4Si. ^{31}P resonances were measured relative to external 85% H_3PO_4. Melting points were obtained in nitrogen-filled tubes on a Mel-Temp capillary apparatus and are uncorrected. Elemental analyses were obtained either on a Carlo Erba Strumentazione Model 1106 elemental analyzer or from Oneida Research Services, Inc., Whitesboro, NY.

[(η^2-cyclenP)Pt(η^2-$Ph_2P(CH_2)_2PPh_2$)]X [X = Cl (2a), PF_6 (2b)]. A stirred solution of 1 (138 mg, 0.200 mmol) in THF (3 mL) was treated dropwise with a solution of dppe (80 mg, 0.20 mmol) in THF (3 mL). After stirring for 6 h, the resulting precipitate was filtered, washed with THF, and pumped dry to yield **2a**, as a white, air-stable solid (155 mg, 93%). Mp: 235–237 °C dec. Anal. Calcd for $C_{34}H_{40}ClN_4P_3Pt$: C, 49.33; H, 4.83; N, 6.77. Found: C, 49.49; H, 4.97; N, 6.30. ^{1}H NMR ($CDCl_3$): δ 2.5–3.2 (comp m, CH_2, 20 H), 7.2–7.6 (comp m, CH, 20 H). **2b** was prepared by treating a stirred solution of **2a** (85 mg, 0.10 mmol) in CH_2Cl_2 (5 mL) dropwise with a solution of $NaPF_6$ (20 mg, 0.11 mmol) in CH_2Cl_2 (2 mL). After stirring for 8 h, the resulting mixture was filtered. The volatiles were pumped off from the filtrate, and the residue was redissolved in CH_2Cl_2 (5 mL). Precipitation with ether yielded **2b** as a white, air-stable solid (92 mg, 92%). Mp: 240–242 °C dec. Anal. Calcd for $C_{34}H_{40}F_6N_4P_4Pt$: C, 43.55; H, 4.30; N, 5.97. Found: C, 43.44; H, 4.86; N, 5.76.

[(H_2cyclenP)Pt(Cl)(η^2-$Ph_2PCH_2PPh_2$)](BF_4)$_2$ (5). A stirred solution of **3** (140 mg, 0.172 mmol) in THF (5 mL) was treated dropwise with 85% $HBF_4{\cdot}O(C_2H_5)_2$ (65 μL, 0.38 mmol). After stirring for 8 h, the resulting precipitate was filtered, washed with THF, and pumped dry to yield **5** as a white, air-stable solid (62 mg, 96%). Mp: 230–232 °C dec. Anal. Calcd for $C_{33}H_{40}B_2ClF_8N_4P_3Pt$: C, 40.04; H, 4.04; N, 5.66. Found: C, 40.63; H, 4.19; N, 5.74. ^{1}H NMR (DMSO-d_6): δ 2.1–3.4 (comp m, NCH_2, 16 H), 4.98 (pseudo-t, PCH_2, $^2J_{PH}$ = 4.5 Hz), 7.5–7.9 (comp m, CH and NH, 22 H). ^{11}B NMR (DMSO-d_6): δ 3.29. Reactions using less than the stoichiometric amount of HBF_4 also led to **5**, in 80–95% yield (based on quantity of HBF_4 added).

(η^2-cyclenP)Pt[Co(CO)$_3$](μ-$Ph_2PCH_2PPh_2$) (6). Na[Co(CO)$_4$] was prepared by a literature method[4] using NaOH (25 mg, 0.62 mmol) and $Co_2(CO)_8$ (34 mg, 0.10 mmol) in THF (5 mL). The resulting solution was filtered and added dropwise to solid **3** (82 mg, 0.10 mmol). The mixture turned yellow immediately and was stirred for 1 h, after which time the ^{31}P NMR spectrum indicated the reaction to be complete. The resulting mixture was filtered and concentrated to about 2 mL. Hexane was layered on top of the solution and allowed to slowly diffuse in, yielding **6** as yellow, air-stable crystals (80 mg, 86%). Mp: 246–248 °C dec. Anal. Calcd for $C_{36}H_{38}CoN_4O_3P_3Pt$: C, 46.91; H, 4.16; N, 6.08. Found: C, 46.06; H, 3.99; N, 6.05. ^{1}H NMR (THF-d_8): δ 2.1–3.5 (comp m, CH_2, 18 H), 7.1–7.6 (comp m, CH, 20 H). IR (THF, cm^{-1}): 1857 (s), 1895 (vs), 1955 (s).

X-ray Structure Determination and Refinement. Colorless crystals of the CH_3CN solvate of **5** were grown from a solution of CH_3CN/THF. Brown crystals of the benzene solvate of **6** were grown from a solution of benzene/hexanes. Crystals were mounted on an automatic Nicolet R_{3m}/V diffractometer. Pertinent crystallographic data are summarized in Table I. The unit cell parameters were determined by a least-squares fit of 25 reflections in the range $15 \le 2\theta \le 25°$. The space group assignments were consistent with systematic absences. Data were corrected for decay and Lorentz polarization effects, as well as for absorption based on ψ-scans. Neutral atom scattering factors and corrections for

Table I. Crystal Data and Data Collection Parameters for 5 and 6

	5	6
formula	$C_{33}H_{40}N_4P_3ClPt{\cdot}2BF_4{\cdot}CH_3CN$	$C_{36}H_{38}N_4O_3P_3CoPt{\cdot}C_6H_6$
fw	1030.8	999.77
color and habit	colorless polyhedra	brown prisms
cryst syst	monoclinic	monoclinic
space group	$P2_1/n$	$P2_1/n$
a (Å)	16.113 (4)	12.119 (4)
b (Å)	13.194 (5)	24.840 (8)
c (Å)	20.500 (8)	13.919 (4)
β (deg)	109.82 (3)	103.20 (2)
V (Å^3)	4100 (2)	4079 (2)
Z	4	4
T (K)	293	293
ρ_{calcd} (g/cm^3)	1.67	1.63
λ (Å)	Mo Kα, 0.71073 (graphite monochromator)	
μ (cm^{-1})	37.06	41.87
crystal dimens (mm)	0.20 × 0.25 × 0.15	0.20 × 0.35 × 0.15
scan mode	ω–2θ	ω–2θ
scan speed (min, max) (deg/min)	3.5, 15.00	5.0, 25.0
scan width (deg)	1.20 plus Kα separation	1.20 plus Kα separation
2θ (min, max) (deg)	3.0, 45.00	3.5, 50.0
no. of measd reflcns	5869	7734
no. of unique reflcns	5397	7178
no. of obsd reflcns	4204 [$I > 3.0\sigma(I)$]	5254 [$I > 2.5\sigma(I)$]
N (parameters)	451	487
std rflcns	3 every 100	3 every 150
cryst decay (%)	2.0	none
transm coeff (max, min)	0.670, 0.610	1.000, 0.431
R_{int} for multiply measd reflcns	0.05	0.016
h range	−17 → 16	0 → 14
k range	0 → 14	0 → 29
l range	0 → 22	−16 → 16
R	0.060	0.032
R_w	0.095	0.039
Δρ (max, min) (e/Å^3)	4.6, −4.25	1.11, −1.54
k[a]	0.0020	0.000678

[a] $R = \sum||F_o| - |F_c||/\sum|F_o|$, $R_w = [\sum w(|F_o| - |F_c|)^2/\sum w(F_o)^2]^{1/2}$, and $w = [\sigma^2(F_o) + k(F_o)^2]^{-1}$.

(3) (a) Lattman, M.; Chopra, S. K.; Burns, E. G. *Phosphorus Sulfur* **1987**, *30*, 185. (b) Lattman, M.; Burns, E. G.; Chopra, S. K.; Cowley, A. H.; Arif, A. M. *Inorg. Chem.* **1987**, *26*, 1926. (c) Khasnis, D. V.; Lattman, M.; Siriwardane, U. *Inorg. Chem.* **1989**, *28*, 681. (d) Khasnis, D. V.; Lattman, M.; Siriwardane, U. *Inorg. Chem.* **1989**, *28*, 2594. (e) Siriwardane, U.; Khasnis, D. V.; Lattman, M. *Acta Crystallogr., Sect. C: Cryst. Struct. Commun.* **1989**, *C45*, 1628. (f) Khasnis, D. V.; Lattman, M.; Siriwardane, U. *Phosphorus, Sulfur Silicon* **1990**, *49/50*, 459.

(4) (a) Edgell, W. F.; Lyford, J., IV *Inorg. Chem.* **1970**, *9*, 1932. (b) Matachek, J. R.; Angelici, R. J.; Schugart, K. A.; Haller, K. J.; Fenske, R. F. *Organometallics* **1984**, *3*, 1038.

Table II. Atomic Coordinates (×10⁴) and Equivalent Isotropic Displacement Coefficients (Å² × 10³) for 5

	x	y	z	U(eq)[a]
Pt	6887 (1)	3588 (1)	3795 (1)	28 (1)
Cl	6686 (3)	2471 (3)	2867 (2)	52 (2)
P(1)	7336 (2)	4870 (3)	3218 (2)	33 (1)
P(2)	6303 (2)	2539 (3)	4446 (2)	35 (1)
P(3)	7027 (2)	4376 (3)	4798 (2)	32 (1)
N(1)	6161 (8)	5413 (11)	2767 (7)	56 (5)
N(2)	7384 (9)	4692 (10)	2424 (7)	50 (6)
N(3)	8589 (8)	4588 (10)	3531 (7)	43 (5)
N(4)	7600 (8)	6019 (9)	3577 (7)	42 (5)
C(1)	5829 (12)	4867 (17)	2081 (9)	79 (9)
C(2)	6578 (12)	4771 (16)	1817 (9)	70 (8)
C(3)	8204 (11)	4469 (13)	2315 (9)	58 (8)
C(4)	8919 (11)	4791 (14)	2953 (9)	56 (7)
C(5)	9004 (11)	5304 (12)	4142 (9)	56 (7)
C(6)	8496 (11)	6269 (12)	3929 (10)	54 (8)
C(7)	6986 (12)	6874 (12)	3339 (9)	57 (8)
C(8)	6285 (14)	6563 (13)	2724 (11)	72 (9)
C(9)	6164 (10)	3608 (10)	4964 (8)	38 (6)
C(10)	7039 (9)	1625 (12)	5012 (8)	44 (6)
C(11)	7479 (13)	992 (14)	4714 (11)	70 (9)
C(12)	8092 (15)	289 (17)	5130 (13)	93 (12)
C(13)	8178 (13)	181 (17)	5808 (13)	81 (10)
C(14)	7743 (14)	852 (15)	6117 (11)	72 (9)
C(15)	7168 (12)	1558 (14)	5695 (9)	58 (8)
C(16)	5251 (9)	1949 (11)	4063 (8)	41 (6)
C(17)	5095 (11)	970 (13)	4214 (8)	50 (7)
C(18)	4245 (15)	555 (17)	3913 (12)	84 (11)
C(19)	3552 (14)	1182 (20)	3468 (12)	85 (11)
C(20)	3734 (11)	2086 (16)	3311 (10)	67 (8)
C(21)	4587 (10)	2526 (15)	3579 (9)	63 (8)
C(22)	6849 (9)	5702 (11)	4895 (7)	35 (6)
C(23)	7538 (11)	6350 (11)	5204 (9)	46 (6)
C(24)	7432 (12)	7364 (12)	5267 (8)	52 (7)
C(25)	6550 (14)	7763 (14)	4962 (10)	67 (9)
C(26)	5846 (12)	7112 (13)	4662 (10)	60 (8)
C(27)	5998 (10)	6093 (12)	4620 (9)	46 (7)
C(28)	8020 (9)	4022 (10)	5492 (7)	31 (5)
C(29)	8128 (10)	4281 (14)	6171 (7)	50 (7)
C(30)	8815 (14)	3878 (16)	6695 (9)	67 (9)
C(31)	9372 (13)	3237 (16)	6616 (10)	63 (8)
C(32)	9292 (10)	2922 (14)	5928 (10)	58 (8)
C(33)	8625 (10)	3315 (12)	5355 (9)	49 (7)
N(1)	−155 (20)	3661 (18)	1834 (17)	126 (17)
C(35)	575 (20)	3463 (18)	2251 (17)	87 (14)
C(34)	1396 (19)	3247 (20)	2700 (17)	132 (17)
B(1)	9988 (15)	7532 (17)	5805 (14)	67 (10)
F(1)	9739 (9)	6592 (11)	5648 (9)	133 (9)
F(2)	9654 (12)	8062 (17)	5236 (11)	176 (12)
F(3)	10905 (7)	7508 (10)	6088 (7)	95 (6)
F(4)	9659 (9)	7927 (17)	6238 (9)	162 (10)
B(2)	3883	5318	3224	124
F(5)	3825	6291	3011	120
F(6)	3190	4776	2834	123
F(7)	4687	4995	3181	120
F(8)	3900	5279	3910	120

[a] Equivalent isotropic U defined as one-third of the trace of the orthogonalized U_{ij} tensor.

Table III. Atomic Coordinates (×10⁴) and Equivalent Isotropic Displacement Coefficients (Å² × 10³) for 6

	x	y	z	U(eq)[a]
Pt	1473 (1)	1735 (1)	4929 (1)	29 (1)
Co	214 (1)	2532 (1)	5461 (1)	36 (1)
P(1)	2000 (1)	1111 (1)	3975 (1)	33 (1)
P(2)	2671 (1)	1707 (1)	6383 (1)	30 (1)
P(3)	1277 (1)	2602 (1)	6954 (1)	31 (1)
N(1)	715 (4)	1516 (2)	3433 (3)	37 (2)
C(1)	−314 (5)	1189 (3)	3236 (5)	53 (3)
C(2)	−13 (6)	687 (3)	3851 (5)	55 (3)
N(2)	1155 (4)	564 (2)	3858 (4)	44 (2)
C(3)	1672 (6)	138 (3)	4532 (6)	63 (3)
C(4)	2919 (7)	161 (3)	4550 (6)	66 (3)
N(3)	3182 (4)	725 (2)	4429 (4)	42 (2)
C(5)	4128 (6)	836 (3)	4000 (5)	55 (3)
C(6)	3849 (5)	1366 (3)	3420 (5)	49 (2)
N(4)	2622 (4)	1384 (2)	3115 (3)	36 (2)
C(7)	2156 (5)	1902 (3)	2738 (5)	47 (2)
C(8)	879 (5)	1859 (3)	2629 (5)	49 (2)
C(11)	−571 (6)	1939 (3)	5366 (5)	49 (2)
O(12)	−1139 (5)	1557 (2)	5349 (4)	71 (2)
C(13)	−739 (6)	3051 (3)	5563 (5)	48 (2)
O(14)	−1306 (5)	3397 (2)	5677 (4)	85 (2)
C(15)	956 (7)	2767 (3)	4614 (6)	60 (3)
O(16)	1390 (6)	2977 (2)	4058 (5)	107 (3)
C(20)	2736 (4)	2345 (2)	7067 (4)	33 (2)
C(21)	4160 (5)	1588 (2)	6372 (4)	36 (2)
C(22)	4711 (6)	1107 (3)	6702 (5)	53 (3)
C(23)	5839 (6)	1048 (3)	6686 (5)	67 (3)
C(24)	6427 (7)	1443 (4)	6330 (6)	70 (3)
C(25)	5862 (6)	1911 (3)	5964 (6)	65 (3)
C(26)	4745 (5)	1985 (3)	5985 (5)	48 (2)
C(31)	2328 (5)	1208 (2)	7232 (4)	38 (2)
C(32)	3053 (6)	1122 (2)	8153 (4)	48 (2)
C(33)	2725 (7)	763 (3)	8807 (5)	64 (3)
C(34)	1697 (9)	504 (3)	8544 (6)	73 (4)
C(35)	979 (7)	592 (3)	7650 (6)	63 (3)
C(36)	1305 (6)	951 (2)	6989 (5)	46 (2)
C(41)	1570 (4)	3302 (2)	7402 (4)	34 (2)
C(42)	1666 (5)	3464 (3)	8362 (5)	41 (2)
C(43)	1854 (5)	3993 (3)	8632 (5)	51 (3)
C(44)	1954 (5)	4371 (3)	7946 (6)	55 (3)
C(45)	1866 (6)	4221 (3)	6985 (6)	59 (3)
C(46)	1684 (6)	3687 (2)	6718 (5)	50 (2)
C(51)	781 (5)	2276 (2)	7962 (4)	35 (2)
C(52)	1476 (6)	2102 (3)	8833 (4)	45 (2)
C(53)	1022 (7)	1844 (3)	9540 (5)	62 (3)
C(54)	−122 (7)	1755 (3)	9377 (6)	61 (3)
C(55)	−827 (6)	1921 (3)	8515 (5)	55 (3)
C(56)	−390 (5)	2170 (2)	7805 (5)	41 (2)
C(61)	3910 (17)	−3 (8)	1133 (9)	183 (11)
C(62)	3089 (24)	313 (6)	1439 (11)	210 (16)
C(63)	2096 (20)	82 (7)	1377 (11)	191 (14)
C(64)	1856 (12)	−411 (6)	1057 (9)	126 (7)
C(65)	2607 (12)	−694 (5)	771 (8)	105 (5)
C(66)	3623 (12)	−510 (5)	820 (8)	111 (6)

[a] Equivalent isotropic U defined as one-third of the trace of the orthogonalized U_{ij} tensor.

anomalous dispersion were from common sources.[5] Full-matrix least-squares refinements were carried out using only the observed reflections (see Table I), the function minimized being $\sum w(|F_o|) - (|F_c|)^2$. The structure was solved by heavy atom methods using the SHELXTL-Plus package[6] and subsequent difference Fourier methods. Final full-matrix least-squares refinement using the observed reflections converged to the R values in the table. Hydrogens on carbon atoms were included in calculated positions using appropriate riding models and fixed isotropic thermal parameters. For **5**, all non-hydrogen atoms were refined anisotropically except for one disordered BF_4 group [B(2)]. The geometry of this group was selected from a best fit to the tetrahedral model with B–F and F–F distances of 1.370 and 2.237 Å, respectively. The disordered BF_4 group was included in the final refinement with fixed positional and thermal parameters. The largest residual, 4.6 e/Å³, shown on the final difference Fourier maps is close to the disordered BF_4 group. H-bonded distances N(1)···F(7) = 2.835 (14) Å, N(3)···F(3) = 2.914 (14) Å. For **6**, all nonhydrogen atoms were refined anisotropically. The largest residual, 1.11 e/Å³, shown on the final difference Fourier maps is close to the platinum atom and likely due to the absorption of the irregular shape of the crystal.

Atomic coordinates and equivalent isotropic thermal parameters for **5** and **6** are given in Tables II and III, respectively.

(5) *International Tables for X-ray Crystallography*; Kynoch Press: Birmingham, England, 1974; Vol. IV.
(6) Sheldrick, G. M. Structure Determination Software Programs. Nicolet Instrument Corp., Madison, WI, 1988.

Results and Discussion

Treatment of **1** with dppe leads to displacement of PPh_3 and Cl^- to give the bisbidentate product, [(η^2-cyclenP)-

Table IV. ^{31}P NMR Data for the Compounds

compd (solv)	δ^a (ppm)			$^2J^a$ (Hz)			$^1J^a$ (Hz)		
	P_a	P_b	P_c	P_aP_b	P_aP_c	P_bP_c	PtP_a	PtP_b	PtP_c
1[b] ($CDCl_3$)	−55	21		2			3612	4702	
2a (Me_2SO-d_6)	−15	40	50	19	447	20	2545	3853	1799
3[b] (THF-d_8)	−50	12	−26	*c*	*c*	77	3508	4702	
4 (THF)	−11	−19	−27	*c*	488	48	*d*	*d*	*d*
5[e] (Me_2SO-d_6)	−19	−43	−43	*c*	752	64	4192	3337	1675
6 (THF)	−26	23	44[f]	28	11	89	3064	4639	

[a] P_a is cyclenP phosphorus, P_b is cis to P_a, and P_c is either trans to P_a or uncomplexed to Pt. [b] Data from ref 3d. [c] Not observed; less than 2 Hz. [d] Not assignable due to impurity peaks. [e] Second-order spectrum; data obtained from NMR spectrum simulation program PANIC. [f] This peak is very broad at ambient temperature; it sharpens to a broad doublet at −75 °C.

Scheme I

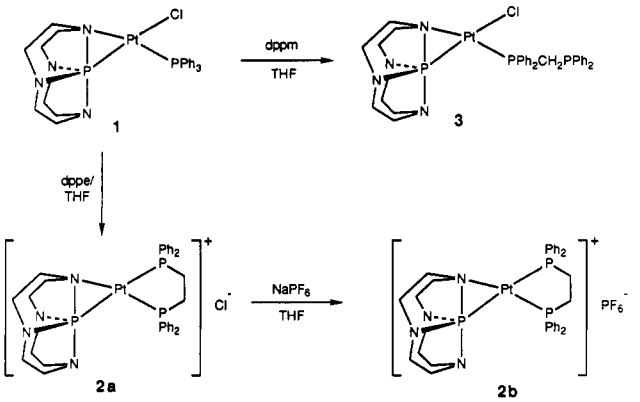

Scheme II

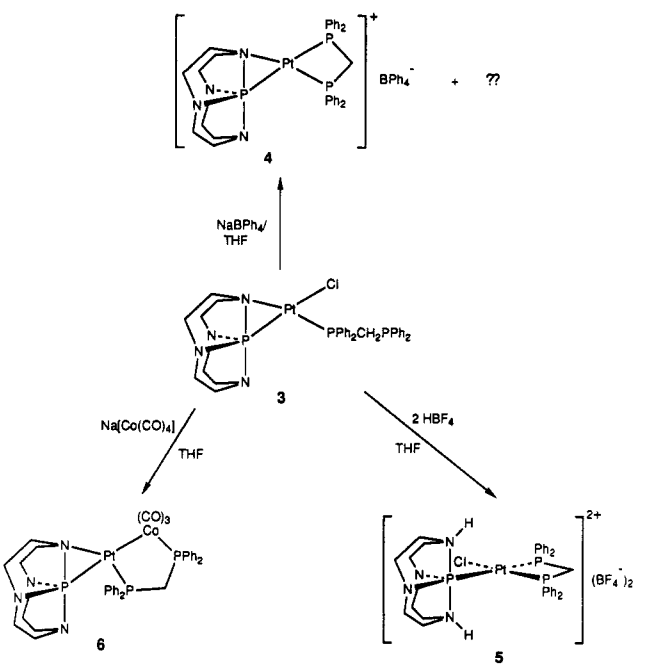

$Pt(\eta^2\text{-}Ph_2P(CH_2)_2PPh_2)]Cl$ (**2a**), in high yield (Scheme I). The identity of **2a** was clearly established by its ^{31}P NMR spectrum, which shows one-bond Pt–P coupling to all three phosphorus atoms (Table IV). In addition, a very large trans P–P coupling and much smaller cis P–P couplings are observed, typical of metal complexes with phosphorus ligands.[7] The ionic nature of **2a** was demonstrated by the ability to replace Cl^- by PF_6^- to give **2b**, which has virtually identical ^{31}P NMR properties (in addition to signals from PF_6^-). This reactivity contrasts markedly with that of dppm, which led to the monodentate dppm complex $(\eta^2\text{-cyclenP})Pt(Cl)Ph_2PCH_2PPh_2$ (**3**).[3d] The ^{31}P spectrum of **3** showed only two signals with one-bond Pt–P couplings. Moreover, only a small P–P coupling through the metal was found, indicative of a cis arrangement of phosphorus atoms.

The inability to bind both ends of dppm in **3** is due, most likely, to the smaller bite angle of dppm (ca. 73°) compared to dppe (ca. 85°). In most cases these differences are not significant since there are large numbers of examples of chelating dppm and dppe complexes.[2] The presence of the η^2-cyclenphosphoranide three-membered ring, with a P–Pt–N angle of ca. 51°, appears to inhibit the formation of a second ring to one having a relatively large angle (i.e., greater than 73°) around the metal. Previous work has shown that, given similar systems, dppe and dppm usually form similar products; when they do not, dppe favors chelate formation while dppm favors bridging structures.[2,8] In this regard **3** is unique since the other end of dppm remains uncoordinated.

Efforts to force the other end of dppm to bind by opening up a coordination site on platinum via chloride abstraction are only partially successful in forming the bischelate species. Dropwise addition of a THF solution of either $NaPF_6$ or $NaBPh_4$ leads to mixtures of products; however, with $NaBPh_4$, a species can be identified in the ^{31}P NMR spectrum as $[(\eta^2\text{-cyclenP})Pt(\eta^2\text{-}Ph_2PCH_2PPh_2)]BPh_4$ (**4**) (Scheme II). The formation of **4** is supported by the large trans P–P coupling (Table IV) and the upfield chemical shifts for both phosphorus atoms of dppm (chelating dppm gives much further upfield ^{31}P chemical shifts than does dppe).[9] Attempts to purify **4** by washing and crystallization led to even more impurities. However, when a coordination site on platinum in **3** is made available by removing the three-membered ring, dppm does form a stable chelate in high yield. Thus, treatment of **3** with HBF_4 [a method previously used to cleave the N–M or N–P bonds in $(\eta^2$-cyclenP)M derivatives] yields $[(H_2cyclenP)Pt(Cl)(\eta^2\text{-}Ph_2PCH_2PPh_2)](BF_4)_2$ (**5**) in which cyclenP is monodentate and dppm bidentate. Here, as in **2**, all three phosphorus atoms show one-bond Pt–P coupling. No monoprotonated adduct of **3** could be isolated (see Experimental Section).

The ability to bind only one end of a usually bidentate ligand should be useful in the preparation of heterobimetallics. Particularly attractive is the possibility of a supported metal–metal bond via chloride displacement utilizing anionic metal carbonyls. In fact, treatment of **3**

(7) (a) Verkade, J. G. *Coord. Chem. Rev.* **1972/1973**, *9*, 1. (b) Pregosin, P. S.; Kunz, R. W. In *NMR, Basic Principles and Progress*; Diehl, P., Fluck, E., Kosfeld, R., Eds.; Springer-Verlag: Berlin, 1979.

(8) (a) Appleton, T. G.; Bennett, M. A.; Tomkins, I. B. *J. Chem. Soc., Dalton Trans.* **1976**, 439. (b) Cooper, S. J.; Brown, M. P.; Puddephatt, R. J. *Inorg. Chem.* **1981**, *20*, 1374.

(9) (a) Crumbliss, A. L.; Topping, R. J. In *Phosphorus-31 NMR Spectroscopy in Stereochemical Analysis*; Verkade, J. G., Quin, L. D., Eds.; VCH: Deerfield Beach, FL, 1987; Chapter 15. (b) Garrou, P. E. *Chem. Rev.* **1981**, *81*, 229.

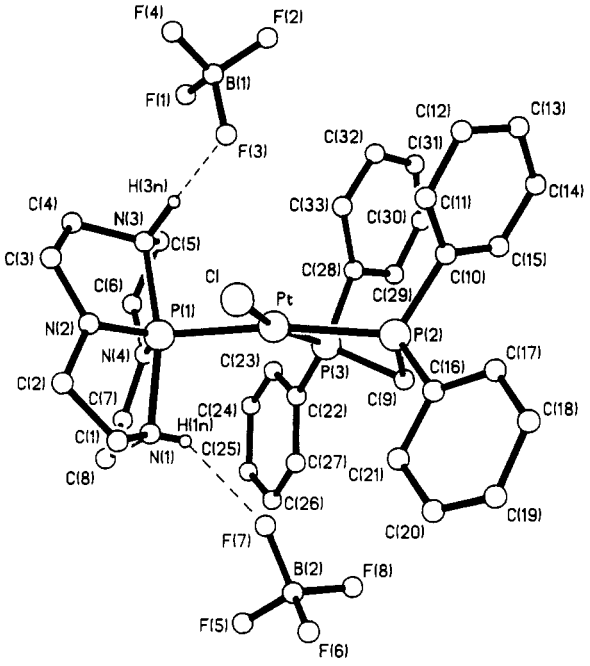

Figure 1. Computer generated drawing of $[(H_2cyclenP)Pt(Cl)(\eta^2\text{-}Ph_2PCH_2PPh_2)](BF_4)_2$ (**5**). Hydrogen atoms (except those involved in H-bonding) omitted for clarity.

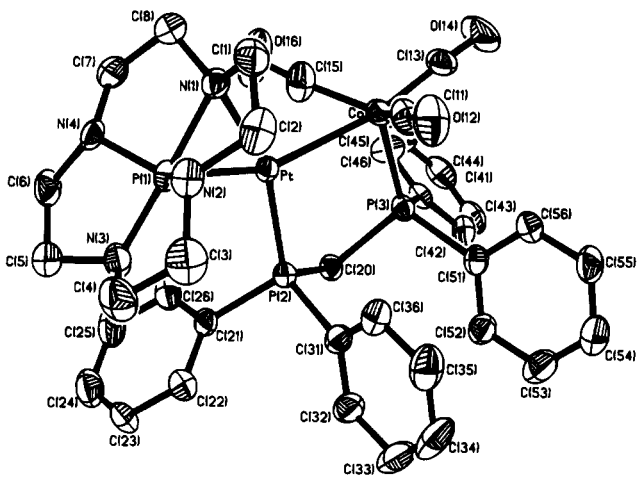

Figure 2. Computer generated drawing of $(\eta^2\text{-cyclenP})Pt[Co(CO)_3](\mu\text{-}Ph_2PCH_2PPh_2)$ (**6**). Hydrogen atoms omitted for clarity.

with $Na[Co(CO)_4]$ leads to $(\eta^2\text{-cyclenP})Pt[Co(CO)_3](\mu\text{-}Ph_2PCH_2PPh_2)$ (**6**) (Scheme II) in which carbon monoxide is eliminated via formation of the dppm bridge. The ^{31}P NMR spectrum of **6** shows that both the cyclenP phosphorus and one end of the dppm are still coordinated to platinum due to the large $^1J_{PtP}$ values; the other end of dppm exhibits a large downfield shift compared to **3**. In addition, the IR spectrum shows three peaks at 1857 (s), 1895 (vs), and 1955 (s). The structure of **6** was confirmed by X-ray crystallography.

The X-ray crystal structures of **5** and **6** were obtained and are illustrated in Figures 1 and 2; selected bond lengths and angles are listed in Table V. The geometry around Pt in **5** is distorted square planar, with the sum of the cis bond angles about the metal 360.2 (3)°. The P(2)–Pt–P(3) angle of 71.7 (1)° is as expected, while the P(2)–C(9)–P(3) angle is 93.9 (9)°. The geometry around P(1) is a distorted trigonal bipyramid (tbp) with N(1) and N(3) at the axial positions and Pt, N(2), and N(4) occupying the equatorial sites. The phosphoranide ligand, H_2cyclenP, is oriented with the P–N equatorial bonds in the platinum coordination plane with Cl–Pt–P(1)–N torsion angles of 89.9 (4) [N(1)], 0.3 (6) [N(2)], −89.2 (4) [N(3)], and 178.8 (5)° [N(4)]. The P–N axial bonds are not only 0.25–0.30 Å longer than the corresponding equatorial bonds but even longer than the sum of the covalent radii. This elongation is due to (1) the usual trend of axial bonds to be longer than equatorial bonds in a tbp and (2) the protonation of the axial nitrogens. Apparently, only the constraint of the cyclen ring around phosphorus prevents rupture of these bonds. Both of the N–H hydrogens are involved in hydrogen bonding to the BF_4^- anions. The geometry around Pt in **6** is distorted square planar, with the sum of the cis bond angles about Pt 360.0 (2)°. The η^2-cyclenP ligand adopts its usual geometry with the N_4P angles close to a tbp geometry and a P(1)–Pt–N(1) angle of 50.4 (1)°. The geometry around Co can be described as a distorted tbp with Pt and C(13) occupying the axial positions and C(11), C(15), and P(3) the equatorial sites.

Table V. Selected Bond Distances (Å) and Angles (deg) for 5 and 6

Compound 5					
Pt–Cl	2.340 (4)	P(1)–N(3)	1.936 (12)	P(1)–N(2)	1.671 (15)
Pt–P(2)	2.332 (4)	Pt–P(1)	2.316 (4)	P(1)–N(4)	1.676 (12)
P(1)–N(1)	1.939 (12)	Pt–P(3)	2.246 (4)		
Cl–Pt–P(1)	91.5 (2)	Cl–Pt–P(2)	96.8 (2)		
P(1)–Pt–P(2)	169.3 (1)	Cl–Pt–P(3)	168.1 (2)		
P(1)–Pt–P(3)	100.2 (1)	P(2)–Pt–P(3)	71.1 (1)		
Pt–P(1)–N(1)	95.1 (5)	Pt–P(1)–N(2)	121.3 (5)		
N(1)–P(1)–N(2)	87.0 (6)	Pt–P(1)–N(3)	99.3 (4)		
N(1)–P(1)–N(3)	165.6 (7)	N(2)–P(1)–N(3)	84.7 (6)		
Pt–P(1)–N(4)	120.9 (5)	N(1)–P(1)–N(4)	86.4 (6)		
N(2)–P(1)–N(4)	117.8 (7)	N(3)–P(1)–N(4)	86.9 (6)		
P(2)–C(9)–P(3)	93.9 (9)				
Compound 6					
Pt–Co	2.704 (1)	P(1)–N(1)	1.863 (5)	Co–C(11)	1.741 (7)
Pt–P(2)	2.206 (1)	P(1)–N(3)	1.718 (5)	Co–C(15)	1.739 (9)
Co–P(3)	2.187 (2)	Pt–P(1)	2.227 (2)	P(1)–N(2)	1.688 (5)
Co–C(13)	1.758 (7)	Pt–N(1)	2.145 (4)	P(1)–N(4)	1.696 (5)
Co–Pt–P(1)	158.3 (1)	Co–Pt–P(2)	93.8 (1)		
P(1)–Pt–P(2)	107.9 (1)	Co–Pt–N(1)	107.9 (1)		
P(1)–Pt–N(1)	50.4 (1)	P(2)–Pt–N(1)	158.3 (1)		
Pt–Co–P(3)	94.1 (1)	Pt–Co–C(11)	72.1 (2)		
P(3)–Co–C(11)	109.4 (2)	Pt–Co–C(13)	168.9 (2)		
P(3)–Co–C(13)	96.9 (2)	C(11)–Co–C(13)	105.6 (3)		
Pt–Co–C(15)	69.4 (2)	P(3)–Co–C(15)	109.5 (2)		
C(11)–Co–C(15)	126.2 (3)	C(13)–Co–C(15)	105.0 (3)		
Pt–P(1)–N(1)	62.5 (2)	Pt–P(1)–N(2)	111.6 (2)		
N(1)–P(1)–N(2)	87.9 (2)	Pt–P(1)–N(3)	119.8 (2)		
N(1)–P(1)–N(3)	177.7 (2)	N(2)–P(1)–N(3)	91.3 (2)		
Pt–P(1)–N(4)	112.2 (2)	N(1)–P(1)–N(4)	87.9 (2)		
N(2)–P(1)–N(4)	127.7 (3)	N(3)–P(1)–N(4)	90.8 (2)		
P(2)–C(20)–P(3)	109.0 (3)				

We have previously shown that ring size and hybridization of the phosphorus atom have significant effects on $^1J_{PtP}$ in related cyclenP systems.[3] Although all of the cyclenP phosphorus atoms are five-coordinate in **1–6**, only in **5** can the entire geometry around P be considered close to a tbp where, to a first approximation, the phosphorus uses an sp^2 hybrid orbital to bond to platinum. This high degree of s-character results in the largest $^1J_{PtP}$ value for the cyclenP phosphorus. In addition, the presence of a phosphorus trans to cyclenP allows the first observation of two-bond trans P–P coupling through Pt with one phosphorus tbp and the other tetrahedral. Here too, **5** shows the largest $^2J_{PP}$ value.[3] Although the larger coupling constants can be attributed to increased s-character in the P–Pt bonds, there is no apparent bond shortening accompanying the hybridization change since the Pt–P(1) and Pt–P(2) bond lengths in **5** are almost identical.

In summary, the present results suggest that a square-planar platinum can easily accommodate both a three-membered and a five-membered ring, while incorporation

of the metal into three- and four-membered rings occurs only with great difficulty. Indeed, while we have been able to find several examples in the literature of square-planar complexes containing both η^2-dppe and η^2-L (η^2-L being a main-group ligand forming a three-membered ring with the metal),[10] we have been unable to locate any corresponding complexes with dppm. Moreover, we have demonstrated the synthetic utility of the constraint of the three-membered ring of η^2-cyclenphosphoranide in the synthesis of a dppm-supported heterobimetallic derivative. This feature may be of general use if other three-membered rings and/or other metals show the same behavior.

Acknowledgment is made to the donors of the Petroleum Research Fund, administered by the American Chemical Society, the Robert A. Welch Foundation, and Southern Methodist University (Seed Grant) for generous financial support. We thank Mr. Harold Isom for help in the synthesis of cyclenPH and Dr. J. P. Fackler for helpful dicussions.

Supplementary Material Available: Tables of anisotropic thermal parameters, bond distances, bond angles, and hydrogen atom coordinates for **5** and **6** (8 pages). Ordering information is given on any current masthead page.

OM910747L

(10) (a) Chatt, J.; Hitchcock, P. B.; Pidcock, A.; Warrens, C. P.; Dixon, K. R. *J. Chem. Soc., Chem. Commun.* **1982**, 932. (b) Werner, H.; Ebner, M.; Otto, H. *J. Organomet. Chem.* **1988**, *350*, 257. (c) Kim, Y.-J.; Osakada, K.; Yamamoto, A. *Bull. Chem. Soc. Jpn.* **1989**, *62*, 964.

Reactivity of Gas-Phase Copper(I) with Octyne Isomers

Denise K. MacMillan and Michael L. Gross*

Midwest Center for Mass Spectrometry, Department of Chemistry, University of Nebraska—Lincoln, Lincoln, Nebraska 68588-0304

Christian Schulze and Helmut Schwarz

Institut für Organische Chemie, Technische Universität Berlin, W 1000 Berlin 12, Germany

Received September 4, 1991

The decompositions of adducts of gas-phase Cu(I) and octyne isomers occur in both tandem and Fourier transform mass spectrometers. Three reactive fragmentations take place for the adducts: hydride abstraction to eliminate copper(I) hydride, propargylic insertion to expel olefins, and remote functionalization to eliminate primarily ethene and hydrogen. A comparison of the abundances of product ions produced in each spectrometer indicates that remote functionalization is a low-energy process, whereas hydride abstraction has the highest energy requirement. The propargylic insertion reaction requires intermediate energy with respect to the other two processes. Second-order reaction rate constants indicate that Cu(I) reacts very efficiently (one of every 2 collisions) with 1- and 3-octyne, but less so with 2- and 4-octyne (one of every 20 collisions).

Introduction

Alkynes are known to be highly reactive with transition metals, and their interactions have been well studied over the last 50 years.[1] Investigation of reactions such as the oligomerization of alkynes catalyzed by transition metals began during World War II with the work of Reppe,[2] but the mechanisms by which these and other metal/alkyne interactions occur are still not well understood. Mass spectrometry is an excellent tool for clarifying gas-phase metal ion–molecule reaction mechanisms because it combines simple, efficient adduct ion formation with sensitive adduct and fragment ion detection. Furthermore, the fragment ions produced by metastable decompositions in a mass spectrometer are indicative of an adduct's lowest energy decomposition pathways.

Gas-phase transition metal ion activation of hydrocarbon C–H and C–C bonds has been demonstrated for many systems by using various mass spectrometric techniques[3] such as tandem mass spectrometry (MS/MS),[4] Fourier transform mass spectrometry (FTMS) and ion cyclotron resonance (ICR) spectrometry,[5] as well as ion beam spectrometry.[6] In many cases, the gas-phase metal ion–molecule interaction involves an oxidative addition

* Author to whom correspondence should be addressed.

(1) Collman, J. P.; Hegedus, L. S.; Norton, J. R.; Finke, R. G. *Principles and Applications of Organotransition Metal Chemistry*; University Science Books: Mill Valley, CA, 1987.

(2) Reppe, W. *Neul Entwicklungen auf dem Gebiete der Chemie des Acetylens und des Kohlenoxyds*; Springer Verlag: New York, 1949.

(3) For reviews of this topic, see: (a) *Gas Phase Inorganic Chemistry*; Russell, D. H., Ed.; Plenum Publishing: New York, 1989. (b) Schwarz, H. *Acc. Chem. Res.* **1989**, *22*, 282. (c) Armentrout, P. B.; Beauchamp, J. L. *Acc. Chem. Res.* **1989**, *22*, 315. (d) Squires, R. R. *Chem. Rev.* **1987**, *87*, 623. (e) Allison, J. In *Progress in Inorganic Chemistry*; Lippard, S. J., Ed.; John Wiley and Sons: New York, 1986; Vol. 34, p 627. (f) Freiser, B. S. *Talanta* **1985**, *32*, 697. (g) Eller, K.; Schwarz, H. *Chem. Rev.* **1991**, *91*, 1121.

(4) (a) Peake, D. A.; Gross, M. L. *Organometallics* **1986**, *5*, 1236. (b) Peake, D. A.; Gross, M. L. *Anal. Chem.* **1985**, *57*, 115. (c) Eller, K.; Zummack, W.; Schwarz, H. *J. Am. Chem. Soc.* **1990**, *112*, 621. (d) Karrass, S.; Schwarz, H. *Organometallics* **1990**, *9*, 2034. (e) Schulze, C.; Schwarz, H. *Int. J. Mass Spec. Ion Processes* **1989**, *88*, 291. (f) Steinruck, N.; Schwarz, H. *Organometallics* **1989**, *8*, 759. (g) Eller, K.; Schwarz, H. *Chimia* **1989**, *43*, 371. (h) Chen, L.; Miller, J. M. *J. Am. Soc. Mass Spectrom.* **1991**, *2*, 120. (i) Tecklenburg, R. E., Jr.; Bricker, D. L.; Russell, D. H. *Organometallics* **1988**, *7*, 2506. (j) Dearden, D. V.; Beauchamp, J. L.; van Koppen, P. A. M.; Bowers, M. T. *J. Am. Chem. Soc.* **1990**, *112*, 9372. (k) van Koppen, P. A. M.; Bowers, M. T.; Beauchamp, J. L. *Organometallics* **1990**, *9*, 625. (l) Karrass, S.; Schwarz, H. *Int. J. Mass Spectrom. Ion Processes* **1990**, *98*, R1.

0276-7333/92/2311-2079$03.00/0